Laser-ultrasonics: principles and industrial applications

Monchalin, Jean-Pierre

Ultrasonic and Advanced Methods for Nondestructive Testing and Material Characterization, pp. 79-121, 2007-05-01

Ultrasonic and Advanced Methods for Nondestructive Testing and Material Characterization, , C.H. Chen editor, World Scientific Publishing Co., 2007

CHAPTER 4

LASER-ULTRASONICS: PRINCIPLES AND INDUSTRIAL APPLICATIONS

Jean-Pierre Monchalin

Industrial Materials Institute, National Research Council of Canada
75, de Mortagne Blvd, Boucherville, Québec, J4B 6Y4, Canada
E-mail: jean-pierre.monchalin@cnrc-nrc.gc.ca

A broad overview of the field of laser-ultrasonics is presented. This overview draws from developments at the Industrial Materials Institute of the National Research Council of Canada as well as elsewhere. The principles of generation and detection are presented, stressing a few key characteristics of laser-ultrasonics: the material is actually the emitting transducer and transduction is made by light, thus eliminating any contact. These features carry both advantages and limitations that are explained. Another feature, which has been an impediment, is actually the complexity of the "laser-ultrasonic transducer", but in spite of this complexity, it can be made very reliable for use in severe industrial environments. It also can be very cost effective for a number of applications. Four applications that are now used in industry are presented: the inspection of polymer matrix composites used in aerospace, the thickness gauging of hot steel tubing in production and the measurement and characterization of thin layers in microelectronics by two different approaches. Technological aspects, such as interferometer design, detection lasers and others are also discussed. As an overall conclusion, laser-ultrasonics that was for a long time a laboratory curiosity has definitely now made its transition to industry. Nevertheless, developments should continue to improve performance, to make it well adapted to specific inspection or characterization tasks and more affordable.

transducer", which is sketched in Fig. 1. As shown in Fig. 1, such a transducer has typically three basic elements, a generation laser, a detection laser and an interferometer, followed by data acquisition and processing electronic hardware. In spite of this complexity, such a transducer can be made very reliable for use in severe industrial environments, as described below. It also can be made very cost effective for a number of applications. Four applications that have now become sufficiently mature for use in industry are described: the inspection of polymer matrix composites used in the aerospace industry, the wall thickness gauging of hot steel tubing in production and the characterization of very thin layers used in the microelectronic industry by two different approaches. Other potential applications that are now being studied in the laboratory or have been demonstrated in industrial conditions are also indicated.

2. Laser Generation of Ultrasound

There are essentially two kinds of mechanisms for generating ultrasound, the first one is perfectly nondestructive and is based on a thermoelastic mechanism (see Fig. 1) while the second one is invasive

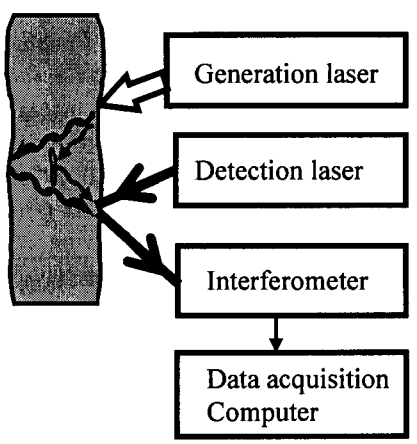

Fig. 1. Sketch of the principle of laser-ultrasonics or of a "laser-ultrasonic transducer".

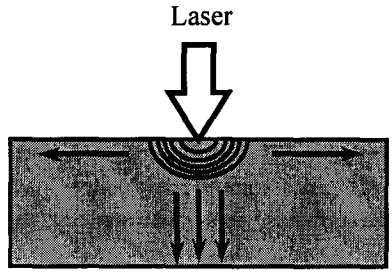

Fig 2. Thermoelastic generation

focusing with a conical lens or axicon), which has the effect of concentrating energy along the axis normal to the surface and passing through the center of the ring (i.e. in other words to focus emitted ultrasound along this axis) [12].

In order to have emission along the normal to the surface in the far field, which is desirable for many applications, there should be some light penetration resulting in a thermoelastic source that is buried underneath the surface. The effect of light penetration can easily be understood by considering the laser heated zone as an ensemble of slices, as shown in Fig. 3a. As shown in Fig. 3b, each slice gives at an observation point inside the medium a displacement compression wavefront first, followed by a displacement rarefaction wavefront after reflection by the free surface and delayed by $2d/V_L$, where d is the slice depth and V_L the longitudinal velocity. These two displacements have opposite polarity but the same magnitude and rise time (equal to the laser pulse duration τ). The actual displacement pulse observed in the medium results from the sum from these two contributions. Therefore, when penetration is very small the displacement pulse is nearly zero, which is the case for metals at frequencies in the range of 1 MHz to about 1 GHz (but not at higher frequencies or for very short pulses, when the typical penetration of 5 to 10 nm for metals becomes comparable to the acoustic wavelength). When penetration increases, the displacement pulse starts to increase and its shape is found to follow proportionally that of the laser pulse. With further increase of light penetration, when the

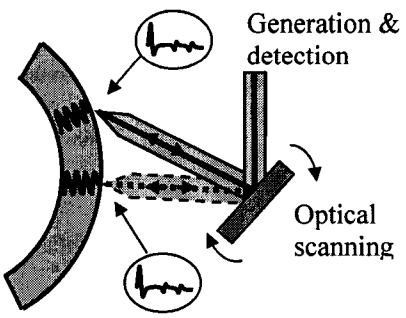

Fig. 4. Effect of penetrating laser light: generation occurs perpendicularly as if a conventional piezoelectric transducer was moved over the surface

in detail with colored glasses giving a wide range of penetration depths [15,18]. Light penetration is very important in practice since its gives a piston source at the surface of the material emitting normally propagating longitudinal waves, independently of the surface curvature and of the orientation of the laser beam. This is at the basis of the inspection of polymer-matrix composites, which is one of the industrial applications of laser-ultrasonics (see Fig. 4).

Enhancement of generation along the normal also occurs when the absorbing material is covered by a transparent layer [19]. In this case, as explained above for the penetrating light source, there are also two delayed and opposite polarity displacement wavefronts that do not cancel if the layer is sufficiently thick. This occurs even if the material has practically no light penetration (metals).

Surface waves and plate waves can also be generated efficiently and in a very versatile manner. When the laser beam is focused to a small circular spot, a surface wave with a cylindrical symmetry is emitted from this spot. Its amplitude has a maximum when the laser pulse duration is about D/V_R where D is the spot diameter and V_R the Rayleigh velocity of the material [20]. Detailed theoretical analysis has been performed and

2.2 *Generation by ablation or vaporization*

If one increases the energy density, particularly for small light penetration (metals), one reaches the threshold where the surface starts to melt and then to get vaporized. At this point, matter is ejected from the surface and through various physical processes this vapor and the surrounding air is ionized, thus producing a plasma plume that expands away from the laser spot on the surface (sketched in Fig. 6). On the opposite surface of a plate-like sample, one first observes a surface elevation spike of duration of the order of the laser pulse duration, which is associated with the recoil effect produced by the matter blown off the surface. This displacement then continues all the time the plasma applies a pressure on the surface and diminishes with plasma expansion and cooling. Therefore, depending upon the energy density, the phenomena taking place goes from solely a vaporization effect for which the ultrasonic pulse has duration of the order of the laser pulse to a strong plasma regime with a much longer duration [4-6]. A similar vaporization effect occurs also when the material is covered by a thin absorbing layer, which is blown off, leaving the substrate underneath substantially unaffected if the energy density is below some threshold. In the strong plasma regime on the other hand, a crater mark is left on the surface (as sketched in Fig. 6). It should also be noted that in addition of vaporization and plasma contributions, there is always some thermoelastic contribution, which is clearly or barely noticeable depending upon the regime.

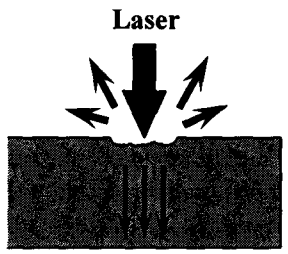

Fig. 6. Generation by ablation or vaporization. In the case of strong ablation, a crater is left on the surface.

motion at a frequency f, simple trigonometric manipulation shows that the backscattered or reflected field includes 3 terms: a central carrier at the laser frequency ν plus two optical sidebands at frequencies ν+f and ν-f. The ratio of the field amplitudes between the sidebands and the central carrier is $2\pi U/\lambda$, where U is the ultrasonic surface displacement amplitude. When the surface motion is not a single frequency, the sidebands are broadened into two symmetric lobes on both sides of the carrier optical frequency ν. These three descriptions of the effect of the surface motion are equivalent and any one could be used to interpret any interferometric detection scheme.

Interferometric detection is based on the conversion by the interferometer of the phase or frequency modulation produced by the surface motion into an intensity modulation, which is detected by the optical detector, as schematically represented in Fig.7 [31,32]. Regarding sensitivity of interferometric detection, it should be noted that there is a fundamental limitation associated with the nature of light as an ensemble of discrete particles. The minimum displacement that can be detected is a function of the number of collected photons and is given by the following formula: $\delta_{lim} = (\lambda/4\pi)\ (B\ h\nu/\ 2\eta P_0)^{1/2}$, where h is the Plank's constant, η the quantum efficiency of the detector, B the electronic

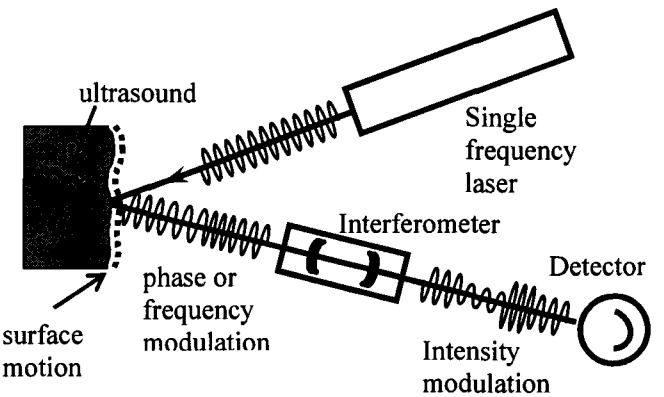

Fig. 7. Principle of optical detection of ultrasound with an interferometer: the interfrometer converts the phase or frequency modulation produced by the surface motion in an intensity modulation.

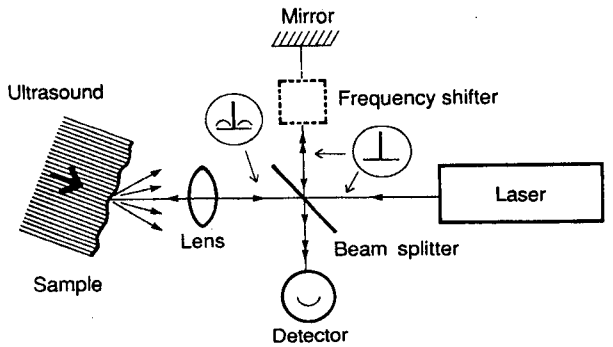

Fig. 8. Michelson interferometer: the inserts indicate schematically the optical spectra along the reference and beam paths.

Still, a more practical scheme is to use the Michelson interferometer as a light filter working as a frequency analyzer of the scattered light [37]. Such a filtering action is obtained by giving very different pathlengths to the two arms of the interferometer. The two interfering waves in the interferometer are then given a time-delay (time-delay interferometry), which should be of the order of half the ultrasonic period for optimum sensitivity. For the frequency range of 1 to 20 MHz, this results into a very bulky system, particularly if immersion in a liquid bath is added to increase etendue. A much more practical implementation of time-delay interferometry and of demodulation by an optical filter is based on the use of multiple beam interference in the confocal Fabry-Perot interferometer.

3.1 *Confocal Fabry-Perot interferometer*

This is a simple optical resonator made of two concave identical mirrors separated by a distance equal to their radius of curvature L_R [38]. As shown in Fig. 9, any incident ray gives 4 rays, two on the transmission side and two in reflection. In excellent approximation each ray retraces its path after multiple reflections in the resonator and the multiple beam interference phenomenon occurs on the 4 output ports. Since this takes

as mentioned above) is valid only at low frequencies (frequencies much below $\Delta\nu_{FP}$). When the frequency increases to about $\Delta\nu_{FP}$, the response levels off and has to be calculated [39,40]. Fig. 11 and 12 show the calculated responsivities and their experimental verification for two confocal Fabry-Perot configurations. In one configuration, the system is used in transmission (detector on the transmission side) and in the other one it is used in reflection (detector on the reflection side, also called sidebands stripping scheme) [41]. The reflection scheme has nearly flat frequency response above $\Delta\nu_{FP}$ (except for the periodic drops every $c/4L_R$) and will be used preferably for detection in this high frequency range. It should be noted that the responsivity is practically zero at very low frequencies, which means that this system is intrinsically insensitive to vibrations, a key advantage for use in industrial environments.

Regarding sensitivity, the minimum detectable displacement is about 4 δ_{lim} at maximum response for the transmission and reflection configurations. When high sensitivity is only required at high frequencies, the back mirror could be made totally reflecting. This leads to improved sensitivity by about a factor two. This can be explained by the fact that the four output beams exiting a confocal cavity, two on the transmission side and another two on the reflection side, giving four independent output ports with multiple interference on each port, are now reduced to two, contributing to an increase of the intensity of interfering terms and consequently of sensitivity. A further improvement by $\sqrt{2}$ can be obtained with a configuration with only a single output port on the reflection side. This can be realized with a totally reflecting back mirror and a front mirror that is totally reflecting over half of its surface, as in the original confocal Fabry-Perot design [33,38]. It should also be noted that the transmission scheme could operate with unpolarized light whereas the use in reflection requires polarizing optics for optimum operation. Therefore often in practice, especially if a large core multimode fiber is used to transmit light to the Fabry-Perot, the transmission configuration gains a sensitivity factor of about $\sqrt{2}$ with respect to the others. If the range of frequencies of interest is between 1 and 15 MHz, which is often the case in nondestructive testing, this configuration will be the one usually selected with a proper choice of

The main weakness of the Fabry-Perot demodulators is their lack of sensitivity at low ultrasonic frequencies (below 2 MHz), which is circumvented by the devices based on two-wave mixing in photorefractive materials described below. Regarding the reduction of the effect of laser noise, a differential scheme which eliminates or at least minimizes laser intensity noise has been reported [42]. More recently another one, more powerful which eliminates in addition phase noise has been described [43].

3.2 *Photorefractive two-wave mixing interferometer*

In the two-wave mixing approach, wavefront adaptation is performed actively, by opposition to the confocal Fabry-Perot in which adaptation is performed by passive or linear optical components; the technique used is also known as real-time holography. This active wavefront adaptation eliminates the need of an external stabilization device against thermal drift or ambient vibrations, as required for the confocal Fabry-Perot. The basic setup of the two-wave mixing interferometer is sketched in Fig. 13. A signal beam which acquires phase shift and speckle after reflection on a surface in ultrasonic motion, is mixed in a photorefractive crystal with a pump plane wave to produce a speckle adapted reference wave that propagates in the same direction as the transmitted signal wave and interferes with it. The quadrature condition is provided by passive optical components after the crystal [44,45].

The etendue, determined by the size of the crystal and the angle between the signal and pump beams, is easily made larger than the etendue of the fiber mentioned above. The response of such a device is flat from a low cut-off frequency f_c , which depends on crystal properties and pump intensity, up to the detector cut-off frequency. There are no periodic sensitivity drops like in the confocal Fabry-Perot. With an InP crystal with proper iron doping, operating at 1.06 μm and with the application of an electric field, the sensitivity is about the same as the maximum sensitivity of the confocal Fabry-Perot used in transmission, i.e. the detection limit is about 4 δ_{lim} [46]. Better sensitivity has been demonstrated with a CdTe crystal with Vanadium doping [47], but CdTe photorefractive crystals need further development before becoming a

reliable source for such a device. At 1.06 μm, GaAs crystals are also used without an electric field giving a sensitivity reduced by about 2.5 compared to the maximum sensitivity of the confocal Fabry-Perot [45,48].

One important advantage of the photorefractive demodulator with respect to the confocal Fabry-Perot is its better sensitivity at low ultrasonic frequencies (below 1 MHz), thus allowing probing more easily materials with strong ultrasonic attenuation (materials with coarse microstructure, porous or mushy materials...). The system has also the advantage to be easily combined with a differential or balanced scheme (two detectors giving responses to phase modulation of opposite sign), so the noise coming from the laser intensity fluctuations can be eliminated to a large extent [49]. Further, by making the pathlengths from the laser to the crystal along the signal and the pump beams to be sensibly equal, the effect of laser phase noise is eliminated.

Its weakness, in spite of the use of semiconductor photorefractive crystals with high photoconductivity (GaAs, InP, CdTe), is its rather slow response time, i.e. the time needed for the photorefractive grating to be built up or to be erased. This affects the ability of the system to adapt to motions of the probed object that cause a change of the speckle pattern of the scattered light or a change of its frequency by the Doppler effect. This time τ_c is related to the low cut-off frequency f_c by the relation $\tau_c = 1/(2\pi f_c)$. The response time also scales essentially as 1/pumping intensity. Responses times as short as 400 ns are obtained at 1.06 μm with an intensity of about 3 kW/cm^2 in a GaAs crystal without an applied electric field. The application of an electric field, which increases sensitivity, has however the drawback to lengthen the response time. With an InP:Fe crystal under a field of 4.9 kV/cm and a power density of about 100 W/cm^2, a time constant of about 2 μs is obtained [46]. These values are longer than those typically obtained with a confocal Fabry-Perot, which can be estimated as $(4\ L_R/c)F$. For a one-meter long Fabry-Perot with a finesse of 10 or a 50 cm long with a finesse of 20, this gives $\tau_c \approx 130$ ns. This means that this system cannot be used as easily as the confocal Fabry-Perot on moving objects. This limitation is illustrated in Fig. 14, which shows the drop of response with the object velocity or Doppler shift (Doppler shift $\Delta\nu = 2V/\lambda$, where V is the projected velocity along the line-of-sight). To be unaffected by a velocity of 1m/s would

3.3 *Imaging and multiplexing with a photorefractive two-wave mixing interferometer*

Any optical receiver that has a sizable etendue can demodulate over several spots in parallel or over an image. Although this can be demonstrated with the confocal Fabry-Perot (using the Connes type to avoid spurious superposition of images), this is more easily implemented with a photorefractive two-wave mixing interferometer. In the multiplex scheme, as shown in Fig. 16, several spots are projected onto the surface of the tested objects according to an arrangement that fits the application (line, grid array, circle...). Scattered light from these spots is then projected onto the photorefractive crystal, either at distinct locations or at the same location from different directions and is finally received by separate detector elements [51,52]. In this last case, it can be shown that there is essentially no cross talk between the various channels when the pump intensity is much larger than the intensity of any signal beam. Such a configuration can obviously be used to increase the speed or

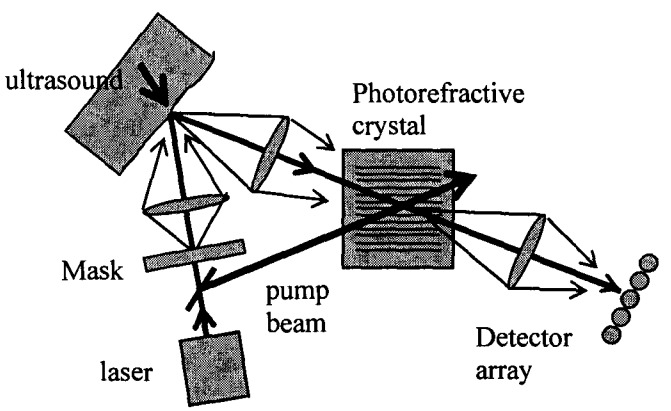

Fig. 16. Sketch of an optical multiplexing scheme associated with a photrefractive demodulator. The mask could be replaced by other optical elements such as an holographic grating or a fiber bundle array to project a light spot distribution onto the surface of the object.

the surface displacement at this point is obtained and could be seen on a CCD camera [53,54].

3.4 *Detection laser*

One key element of the detection scheme is the detection laser. It should be high power, since sensitivity increases with power, and should not contribute to any noise in addition to the fundamental photon or shot noise. High power is particularly needed when the surface is absorbing and detection is at a large distance giving a small collection solid angle. The pulse duration should be sufficiently long to capture all the signal of interest, which means for many applications a duration between 10 and 100μs. Nd-YAG technology at 1.06 μm, which is known to provide high amplification gain, is particularly suited for realizing such a laser by amplifying a small and very stable Nd-YAG laser oscillator [55]. A suitable oscillator is commercially available with power from 100 mW to about 2 W and is based on a small monolithic cavity pumped by a laser diode [56]. Depending upon the repetition rate, the amplifier could be flashlamp pumped (up to 100 Hz) or diode pumped (above 100 Hz) [57]. Faraday isolators are typically used after the small laser oscillator and between amplification stages to prevent feedback and spurious oscillations in such a high gain system. Peak powers of 1 kW and more are typically obtained with pulse duration of the order of 50 μs.

The effect of the additional noise in laser amplifiers that originates from the Amplified Spontaneous Emission (ASE) has been studied for two possible configurations: the amplifier is located ahead of the probed object (pre-amplification scheme) or after it (post-amplification scheme). Pre-amplification is generally preferable because ASE is attenuated by surface absorption and collection losses in the same proportion as the signal beam, making this additional noise negligible in comparison to the shot noise [58].

More recently, since such a master oscillator-pulsed amplifier system is complex and costly, IMI/NRC has been working on the development of a pulsed oscillator without seeding by a low power oscillator. In this system, the laser pulse presents strong relaxation oscillations followed by a plateau of about 100μs with weak residual oscillations. Power of more

generation/detection point from the grid at the origin of the signal. If, after summation a result above a certain noise threshold is obtained, this is indicative of a flaw at the point P. Otherwise there is no flaw at P. Since such processing performed in the time domain can be very computation intensive and fairly long, methods that operate in Fourier space and make use of Fast Fourier Transform algorithms have been developed. These methods, significantly different from the conventional time SAFT, although sometimes called F-SAFT, are based on a plane wave decomposition of the acoustic field for each frequency combined with a back-propagation algorithm [63,64,65]. This processing technique has been applied in particular to the imaging of stress corrosion cracks in steel. One example of the results obtained is shown in Fig. 19 where the crack opening image of stress corrosion cracks in a stainless steel test sample is compared with the image obtained conventionally by liquid penetrants [66]. The laser-ultrasonic image was obtained by scanning the opposite surface and applying an F-SAFT reconstruction algorithm using the laser generated shear waves. It should also be noted that SAFT processing could be applied to laser generated surface and plate waves [67].

5. Industrial applications

We have seen that laser-ultrasonics has been the object of continuous efforts by the scientific and research community to better understand the phenomena taken place during generation and detection of ultrasound and to devise ways to make it usable in an industrial environment. These ways have aimed to push sensitivity, increase bandwidth, insure robustness and reliable operation in spite of ambient disturbances (such as vibrations). However, implementation of the technique is complex, particularly in comparison with conventional piezoelectric-based ultrasonics and also costly and these factors have slowed its industrial use. Nevertheless, we have seen it transitioned during the recent years to the industrial floor for four applications, namely the inspection of aircraft structures made of polymer-matrix composites, the on-line wall thickness gauging of seamless tubes and the thickness determination and characterization of microelectronic thin layers by two approaches.

interesting for inspecting complex parts and for such parts has advantages regarding ease of operation (no additional tooling, no previous detailed knowledge of the part shape, no part precise orientation) and inspection throughput.

This application is first based on the generation of a longitudinal wave normal to the surface independently of the laser beam incident direction, as shown in Fig. 4. As explained above this characteristic is based on the penetration of laser light below the surface for efficient generation and the use of a sufficiently large spot size for minimum ultrasonic beam spreading (5mm typical). For adequate absorption and penetration in these materials, a TEA CO_2 laser operating at 10.6 μm was found quite appropriate and is used in all systems built and presently in use. Penetration is about 20 μm in epoxy and of the same order of magnitude in many paints or peel-plies [13]. Since the system should inspect large areas, a standoff distance of more than one meter is required. This requirement coupled with a scattering surface, which could be also highly absorbing, makes the use of a high power detection laser mandatory. In all the systems developed and presently used, this

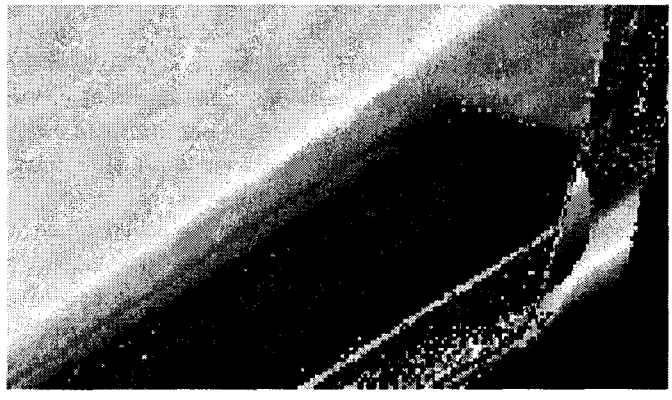

Fig. 20. Laser-ultrasonic C-scan image of part of the horizontal stabilizer of a CF-18 airplane in undismantled and ready for take-off conditions. One will notice that, unlike conventional water jet ultrasonics, laser-ultrasonic allows scanning to the very edge of the part.

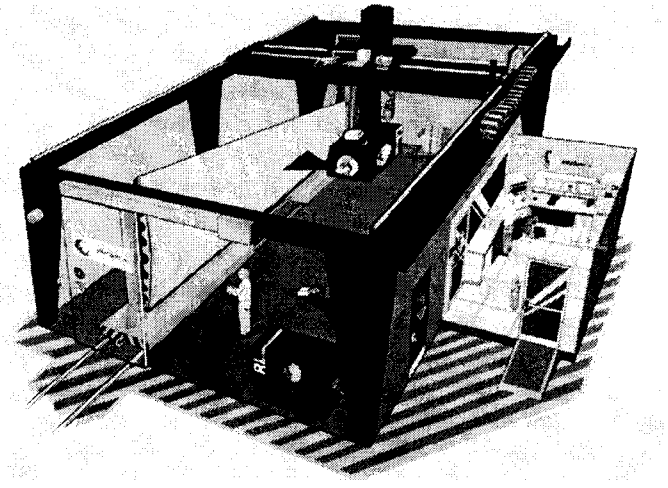

Fig 21. Sketch of the system implemented for the McClellan US Air Force base.

respect to the system installed for the US Air Force make however use of the same concept of a generation unit mounted on a gantry robot [71].

5.2 *On-line wall thickness gauging of seamless tubes*

The development of this application follows from a collaboration between IMI/NRC and the Timken Company, which received the support of the US Department of Energy for the implantation on a Timken production line of a laser-ultrasonic wall thickness gauge. This gauge has now measured reliably since its deployment more than one million tubes [77]. IMI/NRC had demonstrated the feasibility of such an application many years before on a seamless tube production line of Algoma Steel [55,73]. This was also followed by similar demonstrations elsewhere [78].

The use of laser-ultrasonics in this case follows from the need of a sensor for measuring at elevated temperature right on the production line the wall thickness and eccentricity. These tubes are fabricated by hot piercing and are used in particular to make hollow round parts with

cabin houses the lasers, the confocal Fabry-Perot interferometer, control electronics, processing and display data computers. This system also includes a fiber-coupled pyrometer to measure tube temperature and a fiber-coupled coordinate measuring system to determine the measuring locations on the passing tube in rotation and to provide full thickness mapping. A picture of the measuring head on top of the line and above a passing tube is shown in Fig. 23. Note that the implemented system provides eye-safe operation all the time, convenient and fast removal of the measuring head for line service or modification and adequate laser servicing (e.g. periodic flashlamp change) by the location of the lasers in a dust free clean environment. It was also found that the system could provide more than thickness information such as a measurement of the austenitic grain size by proper analysis of ultrasonic attenuation [79]. This application has been commercialized by Tecnar Automation Inc. [80].

5.3 *Thickness determination of microelectronic thin layers*

This industrial application follows from developments performed at Brown University on the generation and detection of very high frequency ultrasound with very short pulse lasers (typically femtosecond Ti:Sapphire lasers with pulse duration of about 100 fs) [81,82]. As shown in Fig. 22, the short pulse laser is directed onto the tested sample, where it generates normally propagating longitudinal waves. We have seen above that such a generation is efficient because the laser pulse is very short, even if light penetration is very small, such as in metals (5 to 10 nm). For such a penetration, the propagation delay though the heated layer is even larger than the pulse duration. Therefore, in practice to resolve very thin layers that are not strongly absorbing, a thin metallic layer has to be added as a transducer layer to insure a sufficiently short pulse. This limitation is not important in practice since the technique is applied essentially to opaque thin films, transparent films being well measured by ellipsometry. The stress pulse is detected by monitoring the change of reflectivity using a stroboscopic technique: as shown in Fig. 22, part of the laser pulse is sent to a delay line and is used to probe the reflectivity change after a given delay. By varying the length of the delay line, the

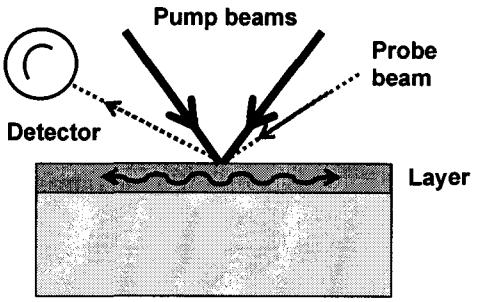

Fig. 23. Sketch of a pump-probe setup based on the transient grating approach.

wavelength. Actually, counter-propagating waves are produced, thus giving a standing surface wave. The time variation of this wave is then monitored by using a probe beam and detecting the beam diffracted by the surface ripple. By varying the angle between the pump beams, the wavelength or k-vector of the surface wave can be changed and its dispersion curve can be measured. Then using suitable modeling, the thickness of the layer and its elastic properties can be determined. This technique has found applications for characterizing films deposited on silicon wafers, such as the thickness measurement of copper interconnections and the determination of the mechanical properties of low permittivity films. It has been commercialized by Philips Advanced Metrology Systems [87].

6. Other Potential Industrial Applications

We have seen that four applications of laser-ultrasonics have made the transition from the laboratory to industry. Many other applications are potential for industrial use and are at various stages of development. Among those, there is the application to the characterization of hot metals during processing. As noted above with respect to the laser-

properties of a paper web and its tension [93,94,95]. The measurement of the thickness of an oil spill from an airplane is also another but challenging application which has been demonstrated [96,97]. The detection of defects at a smaller scale (e.g. on chips or electronic boards) has also been explored and is an application well adapted to laser-ultrasonics by the capability of the technique to provide high frequency ultrasonic testing without water coupling [98].

7. Conclusion

We have presented a broad overview of the basics and of the various technological aspects of laser-ultrasonics. We have outlined the various principles and discussed the phenomena involved in laser generation and detection. We have also presented the advantages and drawbacks of this technique, particularly in comparison with conventional piezoelectric-based ultrasonics. Several of those are linked to the basic characteristic of laser-ultrasonics, which is the use of light as a means for ultrasound emission and detection. Light allows ultrasonic testing without contact and at a distance, thus making possible a wide range of high temperature applications, but sensitivity is on the other hand dependant upon the number of detected photons, which in turn could require a special high power laser for detection (unless the surface has good reflection properties, which is usually the case for microelectronic applications). Many advantages and drawbacks of laser-ultrasonics are also linked to the fact that the material is actually the emitting transducer. This distinguishing feature allows probing more easily parts with complex shapes, but may lead to several limitations depending upon the material, such as very weak emission or material damage. In this regard, we have outlined ways that have been devised to increase the emitted ultrasonic wave amplitude for a specific configuration or task. Detection interferometers well adapted to industrial applications have also been described, including the confocal Fabry-Perot and the two-wave mixing photorefractive interferometer. Since this interferometer has many intrinsic advantages and a remaining drawback, the sensitivity to the Doppler effect associated with object motion having been overcome, it is

9. Scruby, C.B., Dewhurst, R.J., Hutchins, D.A. and Palmer, S.B. "Laser generation of ultrasound in metals", in *Research techniques in Nondestructive testing* , vol. 5, chapter 8, edited by R. S. Sharpe, Academic press, New-York, p. 281.
10. Vogel, J. A., Bruinsma, A. J. A., *Non-destructive testing*, vol.4, eds. J. M. Farley and R. W. Nicols, Pergamon, Oxford, 1988, p. 2267.
11. Noroy, M.-H., Royer, D., Fink, M., "Transient elastic wave generation by an array of thermoelastic sources", *Appl. Phys. Lett.*, **63**, 3276 (1993).
12. Wang, X., Littman, M. G., McManus, J. B., Tadim M., Kimm Y. S., Askarm A., Rabitzm H., "Focused bulk ultrasonic waves generated by ring-shaped laser illumination and application to flaw detection", *J. Appl. Phys.*, **80**, 4274 (1996).
13. Monchalin, J.-P., Choquet, M., Héon, R., Bouchard,P., Padioleau, C., Dubois, M., Enguehard, F., Bertrand, L., Sturrock, W. R., McRae, K. I., "Application of Laser-Ultrasonics to the Inspection of Composite Materials ", Proceedings of the *2nd Canadian International Composites Conference (Cancom '93)*, Sept. 27-29, Ottawa, Ont., eds W. Wallace, R. Gauvin and S. V. Hoa, Canadian Association for Composite Structures and Materials, Montreal, 1993, p. 501.
14. Telshow, K. L., and Conant, R. J., "Optical and thermal parameters effects on laser-generated ultrasound", *J.Acoust. Soc. Am.*, **88**, 1494 (1990).
15. Dubois, M., Enguehard, F. and Bertrand, L., "Analytical one-dimensional model to study the ultrasonic precursor generated by a laser", *Phys. Rev. E*, **50**, 1548 (1994).
16. McDonald, F. A., "Practical quantitative theory of photoacoustic pulse generation", *Appl. Phys. Lett.*, **54**, 1504 (1989).
17. Dubois, M., Enguehard, F., Bertrand, L., Choquet, M., Monchalin, J.-P., " Modeling of laser thermoelastic generation of ultrasound in an orthotropic medium", *Appl. Phys. Lett.*, **64**, 554 (1994).
18. Dubois, M., Enguehard, F., Bertrand, L., Choquet, M., Monchalin, J.-P., "Numerical and experimental studies of the generation of ultrasound by laser", 8th International Topical Meeting on Photoacoustic and Photothermal Phenomena, Pointe-à-Pitre, Guadeloupe, Jan. 22-25 1994, *J.Physique IV*, Colloque C7,vol 4, p.689, (1994).
19. Hutchins, D. A., Dewhurst, R. J. and Palmer, S. B., "Laser generated ultrasound at modified metal surfaces", *Ultrasonics*, **19**, 103 (1981).
20. Arnold, W., Betz, B. and Hoffman, B., "Efficient generation of surface acoustic waves by thermoelesticity", *Appl. Phys. Lett.*, **47**, 672 (1985).
21. Scala, C. M. and Doyle, P. A., "Time- and frequency-domain characteristics of laser-generated ultrasonic surface waves", *J. Acoust. Soc. Am.* , **85**, 1569 (1989).
22. Aindow, A. M., Dewhurst, R. J. and Palmer S. B., "Laser generation of directional surface acoustic wave pulses in metals", *Optics Com.*, **42**, 116 (1982).

Review of Progress in QNDE, vol. 26, eds. D.O. Thompson and D.E. Chimenti, AIP Conference Proceedings, New-York, 2007, in press.

37. Kaule, W., in Proceedings of 8th World NDT conference, Cannes, France, paper 3J5, 1976.
38. Connes, P.,"L'étalon de Fabry-Pérot sphérique" , *J. Physique et le Radium*, **19**, 262 (1958).
39. Monchalin, J.-P., and Héon, R., "Laser ultrasonic generation and optical detection with a confocal Fabry-Perot interferometer", *Materials Evaluation*, **44**, 1231 (1986).
40. Shan, Q., Bradford, A. S. and Dewhurst, R. J., "New field formulas for the Fabry-Perot interferometer and their application to ultrasound detection", *Meas. Sci. Technol.*, **9** , 24 (1998).
41. Monchalin, J.-P., Héon, R., Bouchard, P., Padioleau, C., "Broadband optical detection of ultrasound by optical sideband stripping with a confocal Fabry-Perot", *Appl. Phys. Lett.*, **55**, 1612 (1989).
42. Monchalin J.-P. and Héon, R., "Laser optical ultrasound detection using two interferometer systems", US patent No 5,080,491 (14 Jan. 1992).
43. Blouin, A., Padioleau, C., Néron, C., Lévesque, D. and Monchalin J.-P. , "Differential Confocal Fabry-Perot for the Optical Detection of Ultrasound", in *Review of Progress in QNDE*, vol. 26, eds. D.O. Thompson and D.E. Chimenti, AIP Conference Proceedings, New-York, 2007, in press.
44. Ing, R. K., Monchalin, J.-P., "Broadband optical detection of ultrasound by two-wave mixing in a photorefractive crystal", *Appl. Phys. Lett.* **59**, 3233 (1991).
45. Blouin, A., Monchalin, J.-P., "Detection of ultrasonic motion of a scattering surface by two-wave mixing in a photorefractive GaAs crystal", *Appl. Phys. Lett.*, **65**, 932 (1994).
46. Delaye, P., Blouin, A., Drolet, D., de Montmorillon, L.-A., Roosen, G., Monchalin, J.-P., "Detection of an ultrasonic motion of a scattering surface by photorefarctive InP:Fe under an applied DC field", *J. Opt. Soc. Am.*, **14**, 1723 (1997).
47. de Montmorillon, L.-A., Biaggio, I., Delaye, P., Launay, J.-C., Roosen, G., "Eye-safe large field-of-view homodyne detection using a photorefractive CdTe:V crystal", *Opt. Comm.* **129**, 293 (1996).
48. Drolet, D., Néron, C., Blouin, A. and Monchalin, J.-P., "Specifications of an ultrasonic receiver based on two-wave mixing in photorefractive gallium arsenide implemented in a laser-ultrasonic system", in *Review of Progress in QNDE*, vol. 15, eds. D.O. Thompson and D.E. Chimenti, Plenum, New-York, 1996, p. 637.
49. P. Delaye, A. Blouin, L.-A. de Montmorillon, D. Drolet, J.-P. Monchalin, G. Roosen, "Photorefractive detection of ultrasound", *Proc. SPIE*, **3137**,171, (1997).
50. Campagne, B., Néron, C., Blouin, A. and Monchalin, J.-P., "Doppler frequency-shift compensated photorefractive interferometer for ultrasound detection on

63. Mayer, K., Marklein, R., Langenberg, K. J. and Kreutter, T., "Three-dimensional imaging system based on Fourier transform synthetic aperture focusing technique", *Ultrasonics*, **28**, 241 (1990).
64. Busse, L. J., "Three-dimensional imaging using a frequency-domain synthetic aperture focusing technique", IEEE Transactions **UFFC 39**, 174 (1992).
65. Lévesque, D., Blouin, A., Néron, C. and Monchalin, J.-P., "Performance of laser-ultrasonic F-SAFT imaging", *Ultrasonics*, **40**,1057 (2002).
66. Ochiai, M., Lévesque, D., Talbot, R., Blouin, A., Fukumoto, A. and Monchalin, J.-P., "Visualization of surface-breaking tight cracks by laser-ultrasonic F-SAFT", in *Review of Progress in Quantitative Nondestructive Evaluation*, vol. 22A, eds. D. O. Thompson and D. E. Chimenti, AIP Conference Proceedings, New-York, 2003, p. 1497.
67. Lorraine, P. W., "Laser ultrasonic imaging of Lamb waves in thin plates", in *Review of Progress in Quantitative Nondestructive Evaluation*, vol. 17, eds. D. O. Thompson and D. E. Chimenti , Plenum Press, New-York, 1998, p. 603.
68. Padioleau, C., Bouchard, P., Héon, R., Monchalin, J.-P., Chang, F. H., Drake, T. E. and McRae, K. I., "Laser ultrasonic inspection of graphite epoxy laminates", in *Review of Progress in Quantitative Nondestructive Evaluation*, Vol., 12, eds. D. O. Thompson and D. E. Chimenti, Plenum, New-York, 1993), p. 1345.
69. Chang, F. H., Drake, T. E., Osterkamp, M. A., Prowant, R. S., Monchalin, J.-P., Héon, R., Bouchard. P., Padioleau, C., Froom, D. A., Frazier, W. and Barton, J. P., "Laser ultrasonic inspection of honeycomb aircraft structures" in *Review of Progress in Quantitative Nondestructive Evaluation*, vol. 12, eds. D. O. Thompson and D. E. Chimenti, Plenum, New-York, 1993, p. 611.
70. Drake Jr, T. E., "Review of LaserUT™ Production Implementation", presented at *Review of Progress in Quantitative Nondestructive Evaluation*, Green Bay, Wisconsin, July 27-August 1, 2003, unpublished.
71. Drake Jr, T. E., Dubois, M., Osterkamp, M., Yawn, K., Tho Do, Kaiser, D., Maestas, J. and Thomas, M., "Review of Progress of the LaserUT™ Technology at Lockheed Martin Aeronautics Company", presented at *Review of Progress in Quantitative Nondestructive Evaluation*, Brusnwick, Maine, July 31- August 5, 2005, unpublished.
72. Pétillon, O., Dupuis, J.-P, Voillaume, H., Trétout, H., "Applications of Laser Based Ultrasonics to Aerospace Industry", *Proceedings of the 7th European Conference on Non-Destructive Testing*, Copenhagen, 26-29 May 1998, p.27.
73. Monchalin, J.-P., Néron, C., Bussière, J.F., Bouchard, P., Padioleau, C., Héon, R., Choquet, M., Aussel, J.-D., Carnois, C., Roy, P., Durou, G., Nilson, J.A., "Laser-ultrasonics: from the laboratory to the shop floor", *Advanced Performance Materials*, **5**, 7 (1998).

86. Rogers, J.A., Maznev, A.A., Banet, M.J. and Nelson, K.A., "Optical Generation and Characterization of Acoustic Waves in Thin Films: Fundamentals and Applications", *Ann. Rev. Mater. Sci.*, **30**, 117 (2000).
87. See web site: http://www.advancedmetrologysystems.com.
88. Dubois, M., Moreau, A., Militzer M. and Bussière, J. F., "A New Technique for the Quantitative Real-Time Monitoring of Austenite Grain Growth in Steel", *Scripta Materialia*, **42**, 867 (2000).
89. Lamouche, G., Kruger, S. E., Gille, G., Giguère, N., Bolognini S. and Moreau, A.,"Laser-Ultrasonic Characterization of the Annealing Process of Low-Carbon Steel", in *Review of Progress in Quantitative Nondestructive Evaluation*, vol. 22B, eds. D. O. Thompson and D. E. Chimenti, AIP Conference Proceedings, New-York, 2003, p. 1681.
90. Kruger,S. E., Moreau, A., Militzer M. and Biggs, T., "In-Situ, Laser-Ultrasonic Monitoring of the Recrystallization of Aluminum Alloys" *Thermec 2003 International Conference on Processing & Manufacturing of Advanced Materials*, Part 1. Eds. T. Chandra, J. M. Torralba and T. Sakai., Trans Tech Publications Ltd., Uetikon-Zurich, 2003, p. 483.
91. Fomitchov, P. A., Kromine, A. K., Krishnaswamy, S. and Achenbach, J. D., "Ultrasonic imaging of small surface-breaking defects using scanning laser source technique", in *Review of Progress in Quantitative Nondestructive Evaluation*, vol. 21A, eds. D. O. Thompson and D. E. Chimenti, AIP Conference Proceedings, New-York, 2002, p. 356.
92. Choquet, M., Lévesque, D., Massabki, M., Néron, C., Bellinger, N.C., Forsyth, D., Chapman, C.E., Gould, R., Komorowski, J. P., Monchalin, J.-P., "Laser-ultrasonic detection of hidden corrosion in aircraft lap joints: results from corroded samples", in *Review of Progress in Quantitative Nondestructive Evaluation*, vol. 20A, eds. D. O. Thompson and D. E. Chimenti, AIP Conference Proceedings, New-York, 2001, p. 300.
93. Blouin, A., Reid, B., Monchalin, J.-P., "Laser-ultrasonic Measurements of the Elastic Properties of a Static and a Moving Paper Web and of the Web Tension", in *Review of Progress in Quantitative Nondestructive Evaluation*, vol. 20A, eds. D. O. Thompson and D. E. Chimenti, AIP Conference Proceedings, New-York, 2001, p.271.
94. Ridgway, P. L., Hunt, A. J., Quinby-Hunt, M., Russo, R. E., "Laser-ultrasonics on moving paper", *Ultrasonics*, **37**, 395 (1999).
95. Ridgway, P. L., Russo, R. E., Lafond, E.F., Jackson, T.G., Baum G.A., Zhang, X."Laser Ultrasonic Measurement of Elastic Properties of Moving Paper: Mill Demonstration" in *Review of Progress in QNDE*, vol: 25, eds. D.O. Thompson and D.E. Chimenti, AIP Conference Proceedings, New-York, 2006, ?.